PROCESSING AND CHARACTERIZATION OF TITANIA FILLED EPOXY- GLASS FIBER COMPOSITES

A THESIS SUBMITTED IN PARTIAL FULFILLMENT OF THE REQUIREMENTS
FOR THE DEGREE OF

Master of Technology in Mechanical Engineering

BY

SUBHRAJIT RAY

Roll No: 207ME211

Specialization: Production Engineering

DEPARTMENT OF MECHANICAL ENGINEERING

NATIONAL INSTITUTE OF TECHNOLOGY

ROURKELA 769008

May 2009

PROCESSING AND CHARACTERIZATION OF TITANIA FILLED EPOXY- GLASS FIBER COMPOSITES

A THESIS SUBMITTED IN PARTIAL FULFILLMENT OF THE REQUIREMENTS
FOR THE DEGREE OF

Master of Technology in Mechanical Engineering

BY

SUBHRAJIT RAY

Roll No: 207ME211

Specialization: Production Engineering

Under the guidance of

Prof. Sandhyarani Biswas

DEPARTMENT OF MECHANICAL ENGINEERING

NATIONAL INSTITUTE OF TECHNOLOGY

ROURKELA 769008

May 2009

DEPARTMENT OF MECHANICAL ENGINEERING
NATIONAL INSTITUTE OF TECHNOLOGY
ROURKELA 769008

C E R T I F I C A T E

This is to certify that the thesis entitled **PROCESSING AND CHARACTERIZATION OF TITANIA FILLED EPOXY- GLASS FIBER COMPOSITES** submitted by **Subhrajit Ray** (Roll No. 207 ME 211) in partial fulfillment of the requirements for the award of the degree of **Master of Technology** in Mechanical Engineering with specialization in Production Engineering to the National Institute of Technology, Rourkela is an authentic work carried out under my supervision and guidance.

To the best of my knowledge, the matter embodied in the thesis has not been submitted to elsewhere for the award of any degree.

Place**:** Rourkela
Date**:**

Prof. Sandhyarani Biswas
Mechanical Engineering Department
National Institute of Technology
Rourkela-769008

DEPARTMENT OF MECHANICAL ENGINEERING
NATIONAL INSTITUTE OF TECHNOLOGY
ROURKELA 769008

A C K N O W L E D G E M E N T

It gives me immense pleasure to express my deep sense of gratitude to my supervisor **Prof. Sandhyarani Biswas** for her invaluable guidance, motivation, constant inspiration and above all for her ever co-operating attitude that enabled me in bringing up this thesis in the present form.

I am extremely thankful to **Prof. R. K. Sahoo**, Head, Department of Mechanical Engineering and **Prof. Alok Satapathy** of Mechanical Engineering Department for providing all kinds of possible help and advice during the course of this work.

It is a great pleasure for me to acknowledge and express my gratitude to my parents for their understanding, unstinted support and endless encouragement during my study.

I am greatly thankful to all the staff members of the department and all my well wishers, class mates and friends for their inspiration and help.

Lastly, I sincerely thank to all those who have directly or indirectly helped for the work reported herein.

Date:

SUBHRAJIT RAY

Roll No: 207 ME 211
M. Tech.(Specialization: Production Engg.)
Dept. of Mechanical Engg. , N.I.T., Rourkela

A B S T R A C T

The present work describes the development and characterization of a new set of hybrid polymer composites consisting of glass fibre reinforcement, epoxy resin and TiO_2 particulate fillers. The newly developed composites are characterized with respect to their mechanical and erosion wear characteristics. Experiments are carried out to study the effect of fiber content, impact velocity, impingement angle, stand-off distance and erodent size on the solid particle erosion behaviour of these glass fiber epoxy based hybrid composites. Then the significant control factors and their interactions predominantly influencing the wear rate are identified by using Taguchi method. The study reveals that the fiber content in the composites, impact velocity, impingement angle and erodent size have substantial influence in determining the rate of material loss from the composite surface due to erosion. Also, artificial neural network (ANN) technique has been use to predict the erosion rate based on the experimentally measured database of composites. The morphology of eroded surfaces is examined by using scanning electron microscopy (SEM) and possible erosion mechanisms are discussed.

C O N T E N T S

LIST OF TABLES

LIST OF FIGURES

CHAPTER 1

INTRODUCTION

1.1. Overview of composites

The development of composite materials and related design and manufacturing technologies is one of the most important advances in the history of materials. Composites are multifunctional materials having unprecedented mechanical and physical properties that can be tailored to meet the requirements of a particular application. Many composites also exhibit great resistance to high-temperature corrosion and oxidation and wear. These unique characteristics provide the mechanical engineer with design opportunities not possible with conventional monolithic (unreinforced) materials. Composites technology also makes possible the use of an entire class of solid materials, ceramics, in applications for which monolithic versions are unsuited because of their great strength scatter and poor resistance to mechanical and thermal shock. Further, many manufacturing processes for composites are well adapted to the fabrication of large, complex structures, which allows consolidation of parts, reducing manufacturing costs.

1.1.1. What is Composite Material?

Composite materials are engineering materials made from two or more constituent materials that remain separate and distinct on a macroscopic level while forming a single component. There are two categories of constituent materials: matrix and reinforcement. The matrix material surrounds and supports the reinforcement materials by maintaining their relative positions. The reinforcements impart their special mechanical and physical properties to enhance the matrix properties. The primary functions of the matrix are to transfer stresses between the reinforcing fibers/particles and to protect them from mechanical and/or

environmental damage whereas the presence of fibers/particles in a composite improves its mechanical properties such as strength, stiffness etc. The objective is to take advantage of the superior properties of both materials without compromising on the weakness of either. As defined by Agarwal and Broutman [1] composite means material having two or more distinct constituent materials or phases. It is only when the constituent phases have significantly different physical properties and thus the composite properties are noticeably different from the constituent properties.

1.1.2. Classification of Composites

According to geometry:

Most composite materials developed thus far have been fabricated to improve mechanical properties such as strength, stiffness, toughness, and high temperature performance. It is natural to study together the composites that have a common strengthening mechanism. The strengthening mechanism strongly depends on the geometry of the reinforcement. Therefore, it is quite convenient to classify composite materials on the basis of the geometry of a representative unit of reinforcement. Figure 1.1 represents a commonly accepted classification scheme for composite materials.

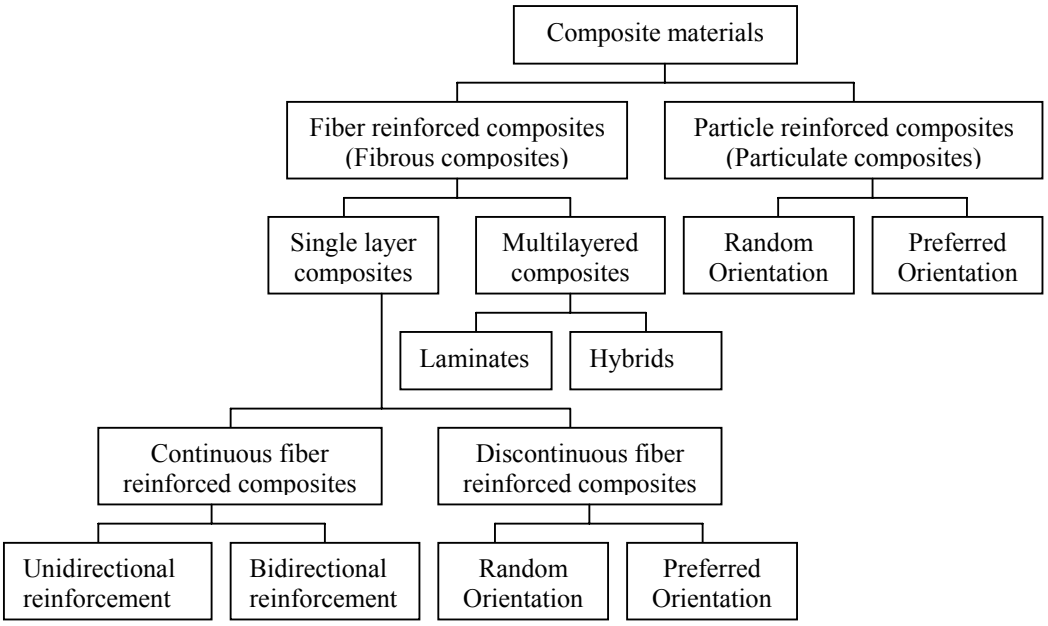

Figure 1.1. Classification of composite materials

Fibrous composite

A fiber is characterized by its length being much greater compared to its cross-sectional dimensions. The dimensions of the reinforcement determine its capability of contributing its properties to the composite. Fibers are very effective in improving the fracture resistance of the matrix since a reinforcement having a long dimension discourages the growth of incipient cracks normal to the reinforcement that might otherwise lead to failure, particularly with brittle matrices. Man-made filaments or fibers of non polymeric materials exhibit much higher strength along their length since large flaws, which may be present in the bulk material, are minimized because of the small cross-sectional dimensions of the fiber. In the case of polymeric materials, orientation of the molecular structure is responsible for high strength and stiffness.

Fibrous composites can be broadly classified as single layer and multi layer composites on the basis of studying both the theoretical and experimental properties. *Single layer composites* may actually be made from several distinct layers with each layer having the same orientation and properties and thus the entire laminate may be considered a single layer composite. Most composites used in structural applications are *multilayered*; that is, they consist of several layers of fibrous composites. Each layer or lamina is a single layer composite and its orientation is varied according to design. Several identical or different layers are bonded together to form a multilayered composites usable for engineering applications. When the constituent materials in each layer are the same, they are called simply *laminates*. *Hybrid* laminates refer to multilayered composites consisting of layers made up of different constituent materials.

Reinforcing fibers in a single layer composite may be short or long compared to its overall dimensions. Composites with long fibers are called *continuous fiber reinforced composites* and those with short fibers, *discontinuous fiber reinforced composites*. The continuous fibers

in single layer composites may be all aligned in one direction to form a *unidirectional composite*. Such composites are fabricated by laying the fibers parallel and saturating them with resinous material. The *bidirectional reinforcement* may be provided in a single layer in mutually perpendicular directions as in a woven fabric. The bidirectional reinforcement may be such that the strengths in two perpendicular directions are approximately equal. The orientation of discontinuous fibers cannot be easily controlled in a composite material. So fibers can be either *randomly oriented* or *preferred oriented*. In most cases the fibers are assumed to be randomly oriented in the composites. However, in the injection molding of a fiber reinforced polymer, considerable orientation can occur in the flow direction and which a case of preferred oriented fibers in the composites.

Particulate Composites

As the name itself indicates, the reinforcement is of particle nature (platelets are also included in this class). It may be spherical, cubic, tetragonal, a platelet, or of other regular or irregular shape, but it is approximately equiaxed. In general, particles are not very effective in improving fracture resistance but they enhance the stiffness of the composite to a limited extent. Particle fillers are widely used to improve the properties of matrix materials such as to modify the thermal and electrical conductivities, improve performance at elevated temperatures, reduce friction, increase wear and abrasion resistance, improve machinability, increase surface hardness and reduce shrinkage. Also, in case of particulate reinforced composites the particle can be either randomly oriented or preferred oriented.

According to type of matrix material they are classified as:

- Metal Matrix Composites (MMC)
- Ceramic Matrix Composites (CMC)
- Polymer Matrix Composites (PMC)

Metal Matrix Composites

Metal Matrix Composites have many advantages over monolithic metals like higher specific modulus, higher specific strength, better properties at elevated temperatures, and lower coefficient of thermal expansion. Because of these attributes metal matrix composites are under consideration for wide range of applications viz. combustion chamber nozzle (in rocket, space shuttle), housings, tubing, cables, heat exchangers, structural members etc.

Ceramic matrix Composites

One of the main objectives in producing ceramic matrix composites is to increase the toughness. Naturally it is hoped and indeed often found that there is a concomitant improvement in strength and stiffness of ceramic matrix composites.

Polymer Matrix Composites

Most commonly used matrix materials are polymeric. The reasons for this are twofold. In general the mechanical properties of polymers are inadequate for many structural purposes. In particular their strength and stiffness are low compared to metals and ceramics. These difficulties are overcome by reinforcing other materials with polymers. Secondly the processing of polymer matrix composites need not involve high pressure and doesn't require high temperature. Also equipments required for manufacturing polymer matrix composites are simpler. For this reason polymer matrix composites developed rapidly and soon became popular for structural applications.

Composites are used because overall properties of the composites are superior to those of the individual components for example polymer/ceramic.

Composites have a greater modulus than the polymer component but aren't as brittle as ceramics.

Two types of polymer composites are:

• Fiber reinforced polymer (FRP)

• Particle reinforced polymer (PRP)

Fiber Reinforced Polymer

Common fiber reinforced composites are composed of fibers and a matrix. Fibers are the reinforcement and the main source of strength while matrix glues all the fibers together in shape and transfers stresses between the reinforcing fibers. The fibers carry the loads along their longitudinal directions. Sometimes, filler might be added to smooth the manufacturing process, impact special properties to the composites, and / or reduce the product cost. Common fiber reinforcing agents include asbestos, carbon / graphite fibers, beryllium, beryllium carbide, beryllium oxide, molybdenum, aluminium oxide, glass fibers, polyamide, natural fibers etc. Similarly common matrix materials include epoxy, phenolic, polyester, polyurethane, peek, vinyl ester etc. Among these resin materials, epoxy is widely used for its higher adhesion and less shrinkage property.

Particle Reinforced Polymer

Particles used for reinforcing include ceramics and glasses such as small mineral particles, metal particles such as aluminium and amorphous materials, including polymers and carbon black. Particles are used to increase the modules of the matrix and to decrease the ductility of the matrix. Particles are also used to reduce the cost of the composites. Reinforcements and matrices can be common, inexpensive materials and are easily processed. Some of the useful properties of ceramics and glasses include high melting temperature, low density, high strength, stiffness, wear resistance, and corrosion resistance. Many ceramics are good electrical and thermal insulators. Some ceramics have special properties; some ceramics are magnetic materials; some are piezoelectric materials; and a few special ceramics are even superconductors at very low temperatures. Ceramics and glasses have one major drawback: they are brittle. An example of particle reinforced composites is an automobile tire, which has carbon black particles in a matrix of poly-isobutylene elastomeric polymer.

1.1.3. Structure of Composite

Structure of composite material determines its properties to a significant extent.

Properties

1) Nature of the constituent material (bonding strength)
2) The geometry of the reinforcement (shape, size)
3) The concentration distribution(vol. fraction of reinforcement)
4) The orientation of the reinforcement(random or preferred)

Good adhesion (bonding) between matrix phase and displaced phase provides transfer of load applied to the material to the displaced phase via the interface. Good adhesion is required for achieving high level of mechanical properties of composites. Very small particles less than 0.25 micrometer finely distributed in the matrix impede movement of dislocations and deformation of the material. They have strengthening effect. Large dispersed phase particles have low share load applied to the material resulting in increase of stiffness and decrease of ductility. Orientation of reinforcement:

- Planar:-In the form of 2-D woven fabric. When the fibers are laid parallel, the composite exhibits axistrope.
- Random or Three Dimensional:-The composite material tends to posses isotropic properties.
- One Dimensional: - Maximum strength and stiffness are obtained in the direction of fiber.

1.1.4. Advantages of Composites

Advantages of composites over their conventional counterparts are the ability to meet diverse design requirements with significant weight savings as well as strength-to-weight ratio. Some advantages of composite materials over conventional ones are as follows:

- Tensile strength of composites is four to six times greater than that of steel or aluminium (depending on the reinforcements).
- Improved torsional stiffness and impact properties.
- Higher fatigue endurance limit (up to 60% of ultimate tensile strength).
- 30% - 40% lighter for example any particular aluminium structures designed to the same functional requirements.
- Lower embedded energy compared to other structural metallic materials like steel, aluminium etc.
- Composites are less noisy while in operation and provide lower vibration transmission than metals.
- Composites are more versatile than metals and can be tailored to meet performance needs and complex design requirements.
- Long life offer excellent fatigue, impact, environmental resistance and reduce maintenance.
- Composites enjoy reduced life cycle cost compared to metals.
- Composites exhibit excellent corrosion resistance and fire retardancy.
- Improved appearance with smooth surfaces and readily incorporable integral decorative melamine are other characteristics of composites.
- Composite parts can eliminate joints / fasteners, providing part simplification and integrated design compared to conventional metallic parts.

1.1.5. Applications of Composites

Table 1.1 shows few applications of composite material in different industry.

Table 1.1. Application of composites

Industry	Examples	Comments
Aircraft	Door, elevators	20-35% Weight savings
Aerospace	Space Shuttle, Space stations	Great weight savings
Automotive	Body frames, engine components	High stiffness & damage tolerance
Chemical	Pipes, Tanks, Pressure vessels	Corrosion resistance
Construction	Structural & decorative panels, Fuel tanks etc.	Weight savings, portable.

1.2. Scope of the project

- The basic aim of the present work is to develop and characterize a new class of composites with epoxy as polymer matrix and glass fiber as the reinforcing material. Their physical and mechanical characterization is done.
- Attempt is made to use TiO_2 as filler in these fiber reinforced polymer matrix composites. Characterization of the resulting TiO_2 filled glass fiber reinforced epoxy composite is done.
- Solid particle erosion wear behaviour of this new class of composites is investigated. Analysis of the experimental results is done using statistical techniques to identify significant control factors affecting the wear properties of these composites.
- The erosion rate based on the experimentally measured database of composites has also been predicted.
- This work is expected to introduce a new class of functional polymer composites suitable for tribological applications.

*****

CHAPTER 2

LITERATURE SURVEY

This chapter outlines some of the recent reports published in literature on composites with special emphasis on erosion wear behaviour of fiber reinforced polymer composites.

Polymer composite materials have generated wide interest in various engineering fields, particularly in aerospace applications. Research is underway worldwide to develop newer composites with varied combinations of fibers and fillers so as to make them useable under different operational conditions. The improved performance of polymer composites in engineering applications by the addition of filler materials has shown a great promise and so has become a subject of considerable interest. Ceramic filled polymer composites have been the subject of extensive research in last two decades. Various kinds of polymers and polymer matrix composites reinforced with ceramic particles have a wide range of industrial applications such as heaters, electrodes [2], composites with thermal durability at high temperature [3] etc. These engineering composites are desired due to their low density, high corrosion resistance, ease of fabrication, and low cost [4-6]. Hard particulate fillers consisting of ceramic or metal particles and fiber fillers made of glass are being used these days to dramatically improve the wear resistance even up to three orders of magnitude [7]. The inclusion of inorganic fillers into polymers for commercial applications is primarily aimed at the cost reduction and stiffness improvement [8, 9]. Along with fiber-reinforced composites, the composites made with particulate fillers have been found to perform well in many real operational conditions. It is reported by Bonner [10] that with the inclusion of micro-sized particulates into polymers, a high filler content (typically greater than 20 vol. %) is generally required to bring the above stated positive effects into play. But at the same time, this may also have detrimental effects on some important properties of the matrix polymers

such as processability, appearance, density and aging performance. It has also been reported that the fracture surface energies of epoxy and polyester resin and their resistance to crack propagation are relatively low [11]. But if particulate filler is added to these resins, the particles inhibit crack growth. As the volume fraction of filler is varied, the fracture energy increases up to a critical volume fraction and then decreases again. Srivastava et al. [12] showed that the fracture toughness of epoxy resin could be improved by addition of flyash particles as filler. The fillers also affect the tensile properties according to their packing characteristics, size and interfacial bonding. The maximum volumetric packing fraction of filler reflects the size distribution and shapes of the particles [13]. Recently, it has been observed that by incorporating filler particles into the matrix of fibre reinforced composites, synergistic effects may be achieved in the form of higher modulus and reduced material costs, yet accompanied with decreased strength and impact toughness.

Polymer composites with both discontinuous and continuous fibre reinforcement possess usually very high specific (i.e. density related) stiffness and strength when measured in plane. Therefore, such composites are frequently used in engineering parts in automobile, aerospace, marine and energetic applications. Due to the operational requirements in dusty environments, the study of solid particle erosion characteristics of the polymeric composites is of high relevance. The resistance of polymers to solid particle erosion has been found to be very poor [14], and in fact it is two or three orders of magnitude lower than metallic materials [15]. One possible way to overcome such a shortcoming is to introduce a hard second phase in the polymer to form polymer matrix composites (PMCs). A number of investigators [14-21] have evaluated the resistance of various types of PMCs to solid particle erosion. Tilly [14] and Tilly and Sage [16] tested nylon and epoxy reinforced with various fibres such as graphite, glass and steel and concluded that the reinforcement can either increase or decrease the erosion resistance depending on the type of fibres. Zahavi et al. [15] tested a number of

PMCs for erosion resistance and concluded that glass-reinforced epoxy composite had a particularly good erosion resistance. Pool et al. [17] conducted erosion tests on four PMCs and inferred that wee-handled, ductile fibres in a thermoplastic matrix exhibit the lowest erosion rates. The above study was extended further by Tsiang [18]. He carried out sand erosion tests on a wide range of thermoset and thermoplastic PMCs having glass, graphite and kevlar fibres in the forms of tape, fabric and chopped mat as reinforcements. Kevlar fibres in an epoxy resin provided the best erosion resistance. In a recent study, Mathias et al. [19] and also Karasek et al. [20] have evaluated the erosion behaviour of a graphite-fibre-reinforced bismaleimide polymer composite. These investigators observed the erosion rates of the PMC to be higher than the unreinforced polymer. Many of the investigators also consistently noted that the erosion rates of the PMCs were considerably larger than those obtained in metallic materials [15-21]. In addition, composites with a thermosetting matrix mostly exhibited a maximum erosion rate at normal impact angles (i.e. a brittle erosion response) while for the thermoplastic polymer composites the erosion rate reached a maximum at an intermediate impact angle in the range 40^0-50^0 signifying a semi-ductile erosion response.

In general, the erosive wear behaviour of material depends on various operating parameters, such as velocity and angle of impact, particle size, shape, flux rate, etc. [22]. Literature on the effect of velocity of erodent on wear performance is sparse as compared to that on other parameters [23-27]. Earlier studies have shown that the value of the velocity exponent depends on the nature of both the target and the erodent. Tilly and Sage [16] reported a value of velocity exponent of 2.3 for 125-150 μm quartz erodents impacting a range of materials from metals to plastics. They also reported that the velocity exponent decreased with decreasing size of the erodent. While studying the erosive wear behaviour of glass eroded by 300 μm size iron spheres, Dhar and Gomes [28, 29] postulated that there was a threshold

velocity value below which deformation was elastic and hence no damage occurred. Tilly [30] proposed that the threshold velocity depended on the particle size of the erodent and obtained a value of 2.7 m/s for 225 μm quartz against 11% chromium steel. Wiederhorn et al. [31] documented the velocity exponents for seven types of target materials having a wide range of brittleness indices and microstructures. Scattergood and Routbort [32] found that the velocity exponent increased with decreasing particle size of the erodent. While studying the erosive wear behaviour of amorphous polystyrene, Thai et al. [33] found that the velocity exponent was 3.69. Karasek et al. [34] observed almost linear correlation between the erosion rate of graphite fibre reinforced bismaleimide composite and the impinging velocity. Arnold and Hutchings [23] found that the erosion rate of natural rubber and epoxidized natural rubber had very strong dependence on the impinging velocity above 70 m/s. Rao et al. [35] reviewed the effect of impact velocity on the erosive wear of various polymers and composites. The influence of impact angle and dose of the erodent on the erosive wear behaviour of various poly-amides with different methylene to amide (CH_2 /CONH) ratio has also been reported [36]. Therefore, it is worthwhile to study the influence of various impact parameters like impinging angle, velocity, dose of the erodent etc. on the erosive wear behaviour of composites. For polymers and composite materials, Tilly and Sage [16] investigated the influence of velocity, impact angle, particle size and weight of impacted abrasive for nylon, carbon-fiber-reinforced nylon, epoxy resin, polypropylene and glass-fiber-reinforced plastic. Fiber reinforcement may improve or worsen the resistance to erosion depending on the type of fibers used. In addition, the erosion rates in composites continued to increase with particle size in contrast with the independence of erosion rate on particle size found in steel with particle diameters greater than about 100 μm [16, 22]. Zahavi and Schmitt [33, 37] performed erosion tests on a quartz-polyimide composite and a quartz-polybutadiene composite and again determined their behaviour to be like that of nearly ideally brittle

materials. One interesting result was the behaviour of an E-glass-reinforced epoxy composite which exhibited erosion rates that were less than those of the other composites by a factor of 5. This was attributed to better adhesion between the matrix and the fibers and the lower porosity of this composite in comparison with the other composites. The E-glass-epoxy composite exhibited semi-ductile erosion behaviour with a maximum weight loss at an impingement angle of 45^0 - 60^0 while the others eroded in a brittle manner with the maximum weight loss occurring at 75^0 - 90^0. The response of materials to solid particle erosion can be categorized as ductile or brittle depending on the variation in the erosion rate (E_r) with impact angle [38-40]. Erosion as well as abrasion experiments on metallic materials, ceramics and polymers have clearly indicated that the hardness of the eroding or abrading material by itself cannot adequately explain the observed behaviour [41-47]. As a result, combined parameters involving both hardness and fracture toughness have been utilized to correlate the erosion data of metals [41], ceramics [45, 46] and polymers [48]. In addition, correlation between the fatigue and the erosion or wear resistance has also been observed in the case of polymers [49].

The erosive wear behaviour of polymer composite systems as a function of fibre content has been studied in the past [50-52]. It was concluded that the inclusion of brittle fibres in both thermosetting and thermoplastic matrices leads to compositions with lower erosion resistance. Nevertheless, no definite rule is available to describe how the fibre content affects the erosion rate of a composite. An analytical approach was presented by Hovis et al. [53] which presumed that the erosion rate of a multiphase material depends on the individual erosion rate of its constituents. The linear (LROM) and inverse (IROM) rules of mixture were proposed and evaluated for a multiphase Al-Si alloy. The same rules of mixture were adopted by Ballout et al. [54] for a glass-fibre reinforced epoxy composite. These two rules of mixture

were also proposed to model the abrasive wear of unidirectional (UD) fibre reinforced composite materials [55, 56].

There are several reports in the literature which discuss the erosion behavior of glass fiber reinforced epoxy composites filled with ceramic fillers. However, very limited work has been done on erosion behavior of glass fiber reinforced epoxy composites filled with Titania (TiO_2). Against this background, the present research work has been undertaken, with an objective to explore the potential of TiO_2 as a filler material in polymer composites and to investigate its effect on the erosion wear performance of the resulting composites. The present work thus aims to develop this new class of particle filled glass fibre composites and to predict their wear behaviour by experimentation. For this, an inexpensive and easy-to-operate experimental strategy based on Taguchi's parameter design has been adopted to study the effect of various control parameters and their interactions.

2.1 Objectives of the Research Work

The objectives of the project are outlined below.

- To study the solid particle erosion behaviour of glass fiber reinforced epoxy based composites filled with TiO_2 particulates filler.
- Evaluation of mechanical properties such as: tensile strength, flexural strength, tensile modulus, micro-hardness, impact strength etc.).
- To identify the significant control factors and their interactions predominantly influencing the erosive wear rate of the composites by using Taguchi experimental design.
- To predict the erosion rate based on the experimentally measured database of composites using artificial neural network (ANN) technique.

******

CHAPTER 3

MATERIALS AND METHODS

This chapter describes the details of processing of the composites and the experimental procedures followed for their characterization and tribological evaluation. The raw materials used in this work are

1. E-glass fiber
2. TiO_2 filler
3. Epoxy resin

3.1. Processing of the Composites

3.1.1. Specimen preparation

E-glass fibers (360 roving taken from Saint Gobian) are reinforced with Epoxy LY 556 resin, chemically belonging to the 'epoxide' family is used as the matrix material. Its common name is Bisphenol A Diglycidyl Ether. The low temperature curing epoxy resin (Araldite LY 556) and corresponding hardener (HY951) are mixed in a ratio of 10:1 by weight as recommended. The epoxy resin and the hardener are supplied by Ciba Geigy India Ltd. E-glass fiber and epoxy resin has modulus of 72.5 GPa and 3.42GPa respectively and possess density of 2590 kg/m^3 and 1100kg/m^3 respectively. The filler material TiO_2 (density 4.2 gm/cm^3) is provided by NICE Ltd India sieved to obtain particle size in the range 70-90 μm. Composites of three different compositions such as 30wt%, 40wt% and 50wt% glass fiber are made and the filler content (weight fraction of TiO_2 in the composite) is kept at 10% for all the samples and the designations of these composites are given in Table 3.1. The castings are put under load for about 24 hours for proper curing at room temperature. Specimens of suitable dimension are cut using a diamond cutter for physical characterization and erosion test.

Table 3.1. Designation of Composites

Composites	Compositions
C_1	Epoxy (60wt%)+Glass Fiber (30wt%)+TiO_2 (10wt%)
C_2	Epoxy (50wt%)+Glass Fiber (40wt%)+TiO_2 (10wt%)
C_3	Epoxy (40wt%)+Glass Fiber (50wt%)+TiO_2 (10wt%)

3.2. Characterization of the Composites

3.2.1. Density

The theoretical density of composite materials in terms of weight fraction can easily be obtained as for the following equations given by Agarwal and Broutman [1].

$$\rho_{ct} = \frac{1}{(W_f/\rho_f)+(W_m/\rho_m)} \quad (1)$$

Where, *W* and ρ represent the weight fraction and density respectively. The suffix f, m and ct stand for the fiber, matrix and the composite materials respectively.

The composites under this investigation consists of three components namely matrix, fiber and particulate filler. Hence the modified form of the expression for the density of the composite can be written as

$$\rho_{ct} = \frac{1}{(W_f/\rho_f)+(W_m/\rho_m)+(W_p/\rho_p)} \quad (2)$$

Where, the suffix '*p'* indicates the particulate filler materials.

The actual density (ρ_{ce}) of the composite, however, can be determined experimentally by simple water immersion technique. The volume fraction of voids (V_v) in the composites is calculated using the following equation:

$$V_v = \frac{\rho_{ct} - \rho_{ce}}{\rho_{ct}} \quad (3)$$

3.2.2. Tensile Strength

The tension test is generally performed on flat specimens as shown in Figure 3.1. The most commonly used specimen geometries are the dog-bone specimen and straight-sided specimen with end tabs. A uni-axial load is applied through the ends. The ASTM standard test recommends that the specimens with fibers parallel to the loading direction should be 11.5 mm wide. Length of the test section should be 100 mm. The test-piece used here was of dog-bone type and having dimensions according to the standards. The tension test was performed on all the three samples as per ASTM D3039-76 test standards.

3.2.3. Flexural Strength

The determination of flexural strength is an important characterization of any structural material. It is the ability of a material to withstand the bending before reaching the breaking point as shown in Figure 3.2a and b. Conventionally a three point bend test is conducted for finding out this material property. In the present investigation also the composites were subjected to this test in a testing machine Instron 1195. The photograph of the machine and the loading arrangement for the specimens are shown in Figure 3.1 and Figure 3.2 respectively. A span of 30 mm was taken and cross head speed was maintained at 10 mm/min. The strength of a material in bending is expressed as the stress on the outermost fibers of a bent test specimen, at the instant of failure. In a conventional test, flexural strength expressed in MPa is equal to:

$$\text{Flexural Strength} = 3PL / 2bd^2$$

Where P= applied central load (N)

L= test span of the sample (m)

b= width of the specimen (m)

d= thickness of specimen under test (m)

3.2.4. Micro-Hardness

Micro-hardness measurement is done using a Leitz micro-hardness tester. A diamond indenter, in the form of a right pyramid with a square base and an angle 136^0 between opposite faces, is forced into the material under a load F. The two diagonals X and Y of the indentation left on the surface of the material after removal of the load are measured and their arithmetic mean L is calculated. In the present study, the load considered F = 24.54N and Vickers hardness number is calculated using the following equation.

$$H_V = 0.1889\frac{F}{L^2} \qquad (4)$$

and $L = \frac{X+Y}{2}$

Where F is the applied load (N), L is the diagonal of square impression (mm), X is the horizontal length (mm) and Y is the vertical length (mm).

Figure 3.1. Experimental set up for three point bend test

Figure 3.2. Loading arrangement for the specimens

3.2.5. Impact strength

Low velocity instrumented impact tests are carried out on composite specimens. The tests are done as per ASTM D 256 using an impact tester (Figure 3.5). The pendulum impact testing machine ascertains the notch impact strength of the material by shattering the V-notched specimen with a pendulum hammer, measuring the spent energy, and relating it to the cross section of the specimen. The standard specimen for ASTM D 256 is 64 x 12.7 x 3.2 mm and the depth under the notch is 10.2 mm as indicted in Figure 3.3.

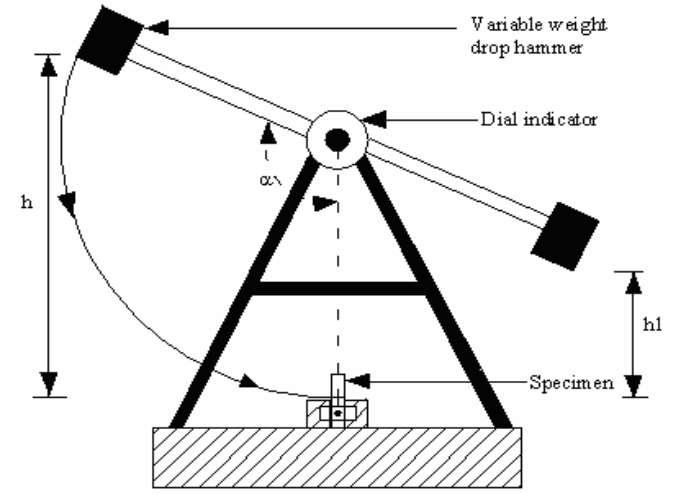

Figure 3.3. Schematic diagram of an impact tester

3.3. Scanning electron microscopy

The surfaces of the composite specimens are examined directly by scanning electron microscope JEOL JSM-6480LV. The samples are washed, cleaned thoroughly, air-dried and are coated with 100 Å thick platinum in JEOL sputter ion coater and observed SEM at 20 kV. Similarly the composite samples are mounted on stubs with silver paste. To enhance the conductivity of the samples, a thin film of platinum is vacuum-evaporated onto them before the photomicrographs are taken.

3.4. Test Apparatus

Figure 3.4 shows the schematic diagram of erosion test rig confirming to ASTM G 76. The set up is capable of creating reproducible erosive situations for assessing erosion wear resistance of the prepared composite samples. It consists of an air compressor, an air particle mixing chamber and an accelerating chamber. Dry compressed air is mixed with the particles which are fed at constant rate from a sand flow control knob through the nozzle tube and then accelerated by passing the mixture through a convergent brass nozzle of 3 mm internal diameter. These particles impact the specimen which can be held at various angles with respect to the direction of erodent flow using a swivel and an adjustable sample clip. The velocity of the eroding particles is measured using double disc method. In the present study, dry silica sand (angular) of different particle sizes (400, 500 and 600 μm) is used as erodent. Each sample is cleaned in acetone, dried and weighed to an accuracy of ±0.1 mg using a precision electronic balance. It is then eroded in the test rig for 30 minutes and weighed again to determine the weight loss. The process is repeated till the erosion rate attains a constant value called steady-state erosion rate. The ratio of this weight loss to the weight of the eroding particles causing the loss is then computed as a dimensionless incremental erosion rate. The erosion rate is defined as the weight loss of the specimen due to erosion divided by the weight of the erodent causing the loss.

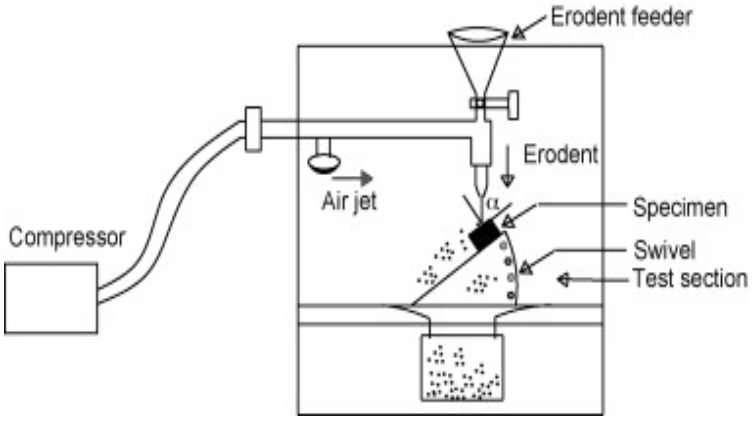

Figure 3.4. Schematic diagram of the erosion test rig

3.5. Taguchi experimental analysis

Design of experiment is a powerful analysis tool for modeling and analyzing the influence of control factors on performance output. The most important stage in the design of experiment lies in the selection of the control factors. Therefore, a number of factors are included so that non-significant variables can be identified at earliest opportunity**.** The wear tests are carried out under operating conditions given in Table 3.2.

Table 3.2. Levels of the variables used in the experiment

Control factor	Level			
	I	II	III	Units
A: Velocity of impact	45	65	85	m/sec
B: Fiber loading	30	40	50	%
C: Stand off distance	120	180	240	mm
D: Impingement angle	30	60	90	degree
E: Erodent size	400	500	600	µm

The tests are conducted at room temperature as per experimental design given in Table 3.3. Five parameters viz., velocity of impact, fiber loading, stand off distance, impingement angle and erodent size each at three levels, are considered in this study in accordance with L_{27} (3^{13}) orthogonal array design. In Table 3.3, each column represents a test parameter and a row gives a test condition which is nothing but a combination of parameter levels. The

experimental observations are transformed into signal-to-noise (S/N) ratios. There are several S/N ratios available depending on the type of characteristics. The S/N ratio for minimum wear rate coming under smaller is better characteristic, which can be calculated as logarithmic transformation of the loss function as shown below.

Smaller is the better characteristic: $\frac{S}{N} = -10 \log \frac{1}{n}\left(\sum y^2\right)$ (5)

where n is the number of observations, and y is the observed data. "Lower is better" (LB) characteristic, with the above S/N ratio transformation, is suitable for minimization of wear rate.

Table 3.3. Orthogonal array for L_{27} (3^{13}) Taguchi's Experimental Design

$L_{27}(3^{13})$	1 A	2 B	3 $(AxB)_1$	4 $(AxB)_2$	5 C	6 $(BxC)_1$	7 $(BxC)_2$	8 $(AxC)_1$	9 D	10 E	11 $(AxC)_2$	12	13
1	1	1	1	1	1	1	1	1	1	1	1	1	1
2	1	1	1	1	2	2	2	2	2	2	2	2	2
3	1	1	1	1	3	3	3	3	3	3	3	3	3
4	1	2	2	2	1	1	1	2	2	2	3	3	3
5	1	2	2	2	2	2	2	3	3	3	1	1	1
6	1	2	2	2	3	3	3	1	1	1	2	2	2
7	1	3	3	3	1	1	1	3	3	3	2	2	2
8	1	3	3	3	2	2	2	1	1	1	3	3	3
9	1	3	3	3	3	3	3	2	2	2	1	1	1
10	2	1	2	3	1	2	3	1	2	3	1	2	3
11	2	1	2	3	2	3	1	2	3	1	2	3	1
12	2	1	2	3	3	1	2	3	1	2	3	1	2
13	2	2	3	1	1	2	3	2	3	1	3	1	2
14	2	2	3	1	2	3	1	3	1	2	1	2	3
15	2	2	3	1	3	1	2	1	2	3	2	3	1
16	2	3	1	2	1	2	3	3	1	2	2	3	1
17	2	3	1	2	2	3	1	1	2	3	3	1	2
18	2	3	1	2	3	1	2	2	3	1	1	2	3
19	3	1	3	2	1	3	2	1	3	2	1	3	2
20	3	1	3	2	2	1	3	2	1	3	2	1	3
21	3	1	3	2	3	2	1	3	2	1	3	2	1
22	3	2	1	3	1	3	2	2	1	3	3	2	1
23	3	2	1	3	2	1	3	3	2	1	1	3	2
24	3	2	1	3	3	2	1	1	3	2	2	1	3
25	3	3	2	1	1	3	2	3	2	1	2	1	3
26	3	3	2	1	2	1	3	1	3	2	3	2	1
27	3	3	2	1	3	2	1	2	1	3	1	3	2

The standard linear graph, as shown in Fig. 3.5, is used to assign the factors and interactions to various columns of the orthogonal array [57].

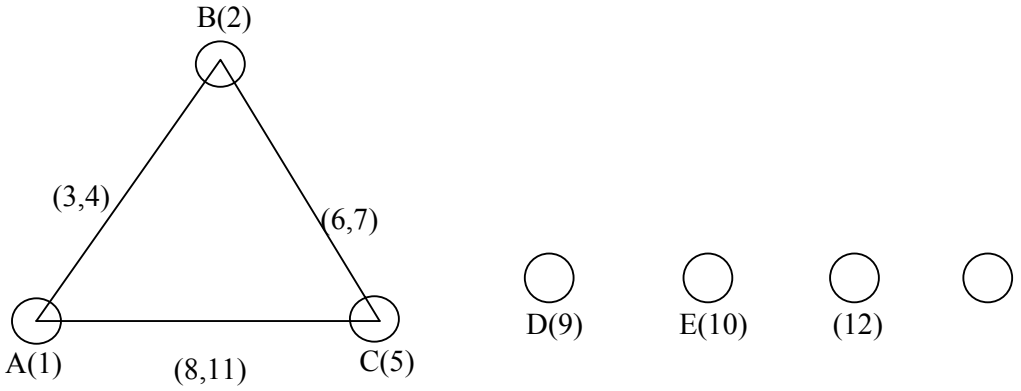

Figure 3.5. Linear graphs for L_{27} array

The plan of the experiments is as follows: the first column is assigned to impact velocity (A), the second column to fiber loading (B), the fifth column to stand-off distance (C), ninth column to impingement angle (D) and twelfth column to erodent size (E), the third and fourth column are assigned to $(A\times B)_1$ and $(A\times B)_2$, respectively to estimate interaction between impact velocity (A) and fiber loading (B), the sixth and seventh column are assigned to $(B\times C)_1$ and $(B\times C)_2$ respectively, to estimate interaction between the fiber loading (B) and stand-off distance (C), the eighth and eleventh column are assigned to $(A\times C)_1$ and $(A\times C)_2$ respectively, to estimate interaction between the impact velocity (A) and stand-off distance (C). The remaining columns are assigned to error columns respectively.

3.6. Neural Computation

Erosion wear process is considered as a non-linear problem with respect to its variables: either materials or operating conditions. To obtain minimum wear rate, combinations of operating parameters have to be planned. Therefore a robust methodology is needed to study these interrelated effects. In this work, a statistical method, responding to the constraints, is implemented to correlate the operating parameters. This methodology is based on artificial neural networks (ANN), which is a technique that involves database training to predict input-

output evolutions. The details of this methodology are described by Rajasekaran and Pai [58]. In the present analysis, the velocity of impact, filler content, stand-off distance, impingement angle and erodent size are taken as the five input parameters. Each of these parameters is characterized by one neuron and consequently the input layer in the ANN structure has five neurons. The database is built considering experiments at the limit ranges of each parameter. Experimental result sets are used to train the ANN in order to understand the input-output correlations. The database is then divided into three categories, namely: (i) a validation category, which is required to define the ANN architecture and adjust the number of neurons for each layer. (ii) a training category, which is exclusively used to adjust the network weights and (iii) a test category, which corresponds to the set that validates the results of the training protocol. The input variables are normalized so as to lie in the same range group of 0-1. The outer layer of the network has only one neuron to represent wear rate. To train the neural network used for this work, about 135 data sets obtained during erosion trials on different composites are taken. Different ANN structures (Input-Hidden-Output nodes) with varying number of neurons in the hidden layer are tested at constant cycles, learning rate, error tolerance, momentum parameter, noise factor and slope parameter. Based on least error criterion, one structure, shown in Table 3.4, is selected for training of the input-output data. Neuron number in the hidden layer is varied and in the optimized structure of the network, this number is 12 for a typical case. The number of cycles selected during training is high enough so that the ANN models could be rigorously trained.

A software package NEURALNET for neural computing developed by Rao and Rao [59] using back propagation algorithm is used as the prediction tool for erosion wear rate of different composites under various test conditions. The three-layer neural network having an input layer (I) with five input nodes, a hidden layer (H) with twelve neurons and an output layer (O) with one output node employed for this work is shown in Fig. 3.6.

Table 3.4. A typical case of Input parameters selected for training

Input Parameters for Training	Values
Error tolerance	0.01
Learning rate (ß)	0.01
Momentum parameter(α)	0.03
Noise factor (NF)	0.01
Number of epochs	20,0000
Slope parameter (£)	0.6
Number of hidden layer	12
Number of input layer neuron (I)	5
Number of output layer neuron (O)	1

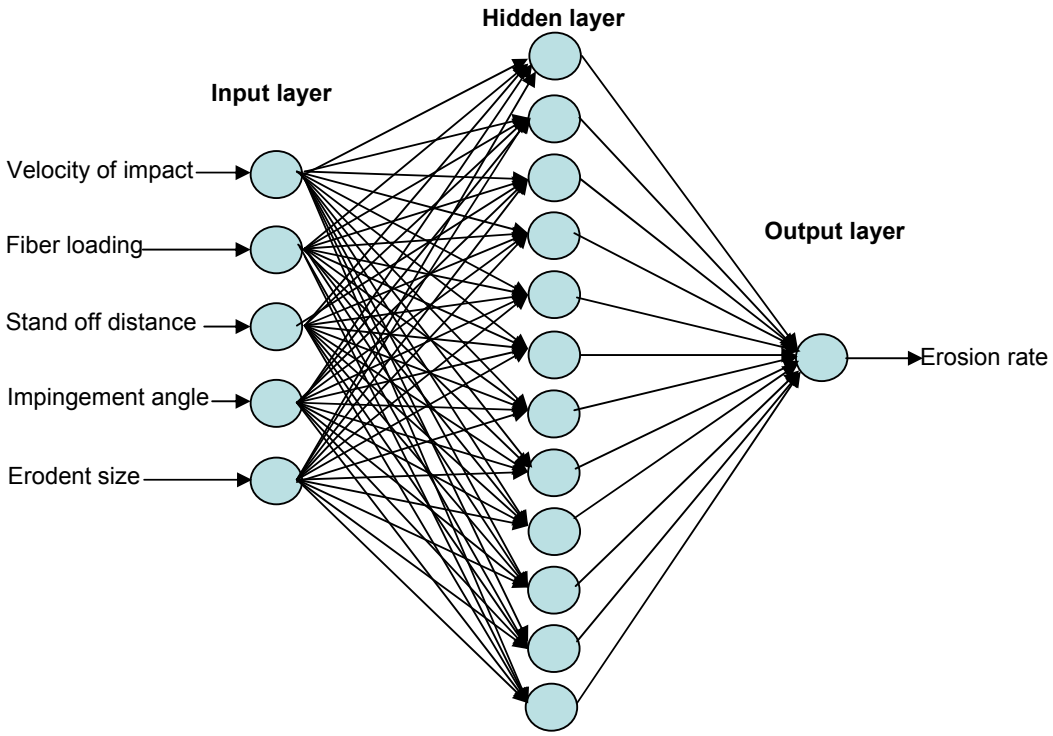

Figure 3.6. Neural network architecture

*****

CHAPTER 4

MECHANICALCHRACTERISTICS OF COMPOSITES: RESULTS & DISCUSSIONS

This chapter presents the physical and mechanical properties of the glass fiber reinforced epoxy composites prepared for this present investigation. Details of processing of these composites and the tests conducted on them have been described in the previous chapter. The results of various characterization tests are reported here. This includes evaluation of tensile strength, flexural strength, measurement of density and micro-hardness has been studied and discussed. The interpretation of the results and the comparison among various composite samples are also presented.

4.1. Mechanical Characteristics of Composites

4.1.1. Density and volume fraction of voids

The theoretical and measured densities of the composites along with the corresponding volume fraction of voids are presented in Table 4.1. It may be noted that the composite density values calculated theoretically from weight fractions using Eq. (3) are not equal to the experimentally measured values. This difference is a measure of voids and pores present in the composites.

Table 4.1 Measured and Theoretical densities of the composites

Composites	Measured density (gm/cc)	Theoretical density (gm/cc)	Volume fraction of voids (%)
C_1	1.429	1.457	1.92
C_2	1.542	1.577	2.21
C_3	1.667	1.719	3.02

Density of a composite depends on the relative proportion of matrix and reinforcing materials and this is one of the most important factors determining the properties of the composites. The void content is the cause for the difference between the values of true density and the theoretically calculated one. The voids significantly affect some of the mechanical properties and even the performance of composites in the workplace. Higher void contents usually mean lower fatigue resistance, greater susceptibility to water penetration and weathering. The knowledge of void content is desirable for estimation of the quality of the composites. It is understandable that a good composite should have fewer voids. However, presence of void is unavoidable in composite making particularly through hand-lay-up route.

The characterization of the composites reveals that inclusion of any particulate filler has strong influence on the physical and mechanical properties of composites. The modified values of the properties of the composites under this investigation are presented in Table 4.2.

Table 4.2. Mechanical properties of the composites

Composites	Hardness (Hv)	Tensile strength (MPa)	Tensile modulus (GPa)	Flexural strength (MPa)	Impact energy (J)
C_1	44	253.3	10.39	161.8	2.4
C_2	49	260.2	8.23	175.7	2.8
C_3	52	308.3	8.77	220.1	3.1

4.1.2. Effect of Fiber loading on Micro-hardness

The measured hardness values of all the three composites are presented in Figure 4.1. It can be seen that the hardness is increasing with the increase in fiber loading at constant filler content. In case of composites with fiber loading up to 50 wt% gives higher value of micro-hardness as compared to 30wt% composite. When the increase in fiber loading the formation of air bubbles and void in composites decreases causing homogeneity in microstructure and affect the mechanical properties.

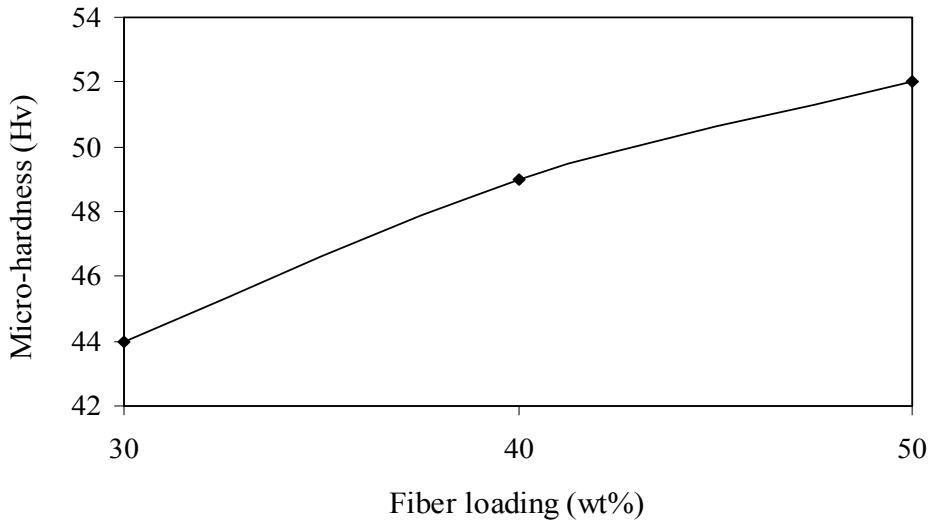

Figure 4.1.Variation of micro-hardness of the composites with the fiber content

4.1.3. Effect of Fiber loading Tensile Properties

The test results for tensile strengths and moduli are shown in Figures 4.2 and 4.3, respectively. It is seen that in all the samples irrespective of the constant filler material the tensile strength of the composite increases with increase in fiber loading. There can be two reasons for this increase in the strength properties of these composites compared. One possibility is that the chemical reaction at the interface between the filler particles and the matrix may be too strong to transfer the tensile stress; the other is that at constant filler content with the increase in fiber loading result in stress concentration in the glass fiber reinforced epoxy composite. These two factors are responsible for increase in the tensile strengths of the composites so significantly. From Figure 4.3 it is clear that with the increase in fiber loading the tensile moduli of the glass epoxy composites decreases gradually.

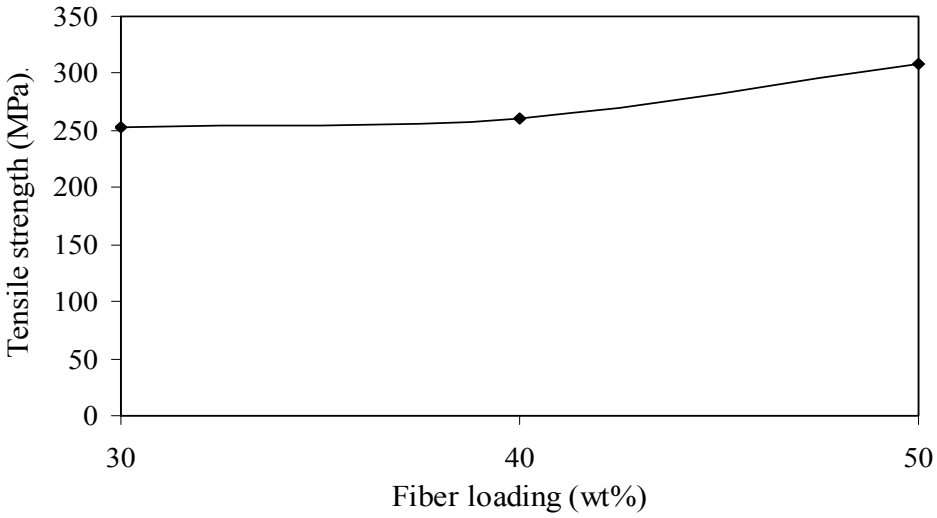

Figure 4.2. Effect of fiber loading on tensile strength of composites

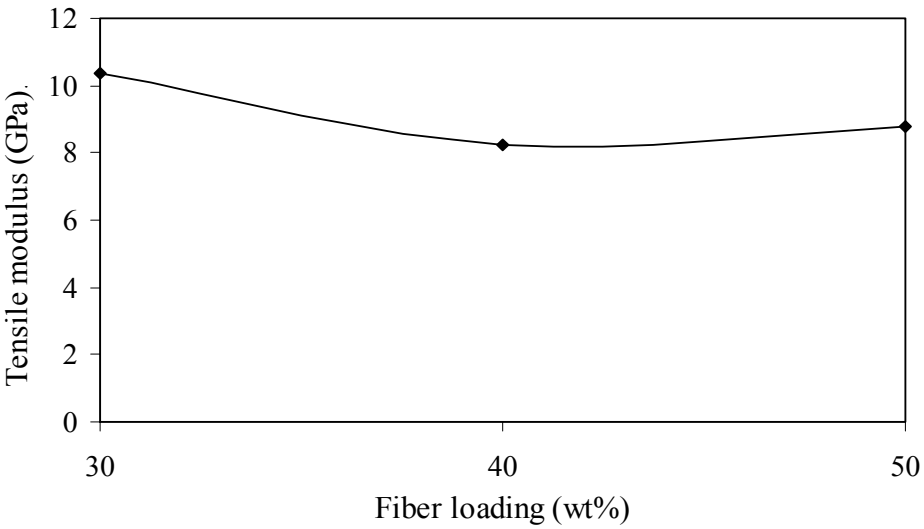

Figure 4.3. Effect of fiber loading on tensile modulus of composites

4.1.4. Effect of Fiber loading Flexural Strength

Figure 4.4 shows the comparison of flexural strengths of the composites obtained experimentally from the bend tests. It is interesting to note that flexural strength increases with increase in fiber loading from 30-50wt% of glass epoxy composite structure.

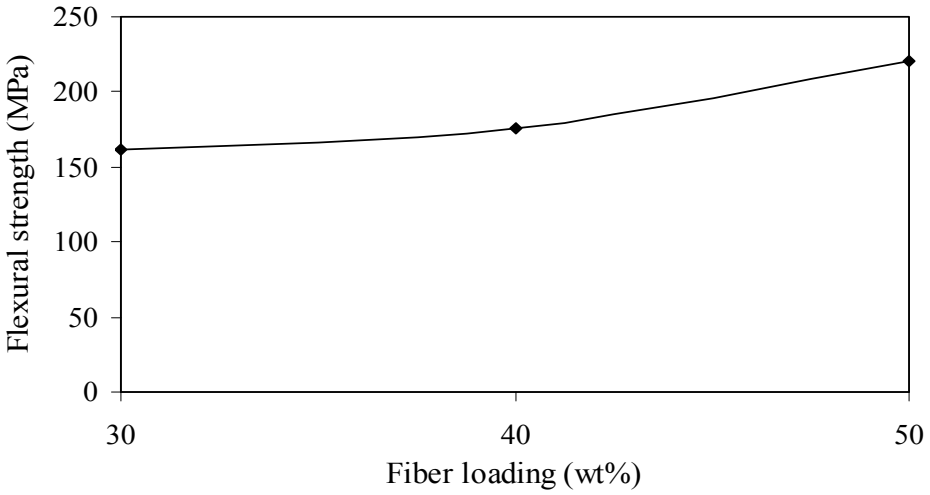

Figure 4.4. Effect of fiber loading on flexural strength of composites

4.1.5. Effect of Fiber loading Impact Strength

The impact energy values of different composites recorded during the impact tests are given in Table 4.1. It shows that the resistance to impact loading of glass epoxy composites improves with increase in fiber loading as shown in Figure 4.5. High strain rates or impact loads may be expected in many engineering applications of composite materials. The suitability of a composite for such applications should therefore be determined not only by usual design parameters, but by its impact or energy absorbing properties.

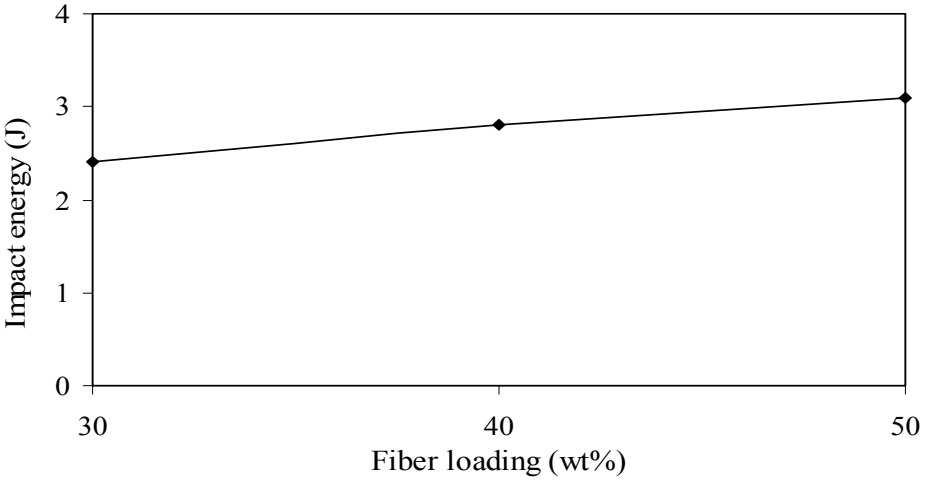

Figure 4.5. Effect of fiber loading on impact strength of composites

CHAPTER 5

EROSION CHARACTERISTICS OF COMPOSITES: RESULTS & ANALYSIS

Statistical methods are commonly used to improve the quality of a product or process. Such methods enable the user to define and study the effect of every single condition possible in an experiment where numerous factors are involved. Solid particle erosion is such a process in which a number of control factors collectively determine the performance output i.e the erosion rate. Hence, in the present work a statistical technique called Taguchi method is used to optimize the process parameters leading to minimum erosion of the polymer composites under study. This part of the chapter presents the Taguchi experimental design methodology in detail. Also artificial neural network technique is applied to predict the erosion rate of composites.

5.1. Experimental analysis

From Table 5.1, the overall mean for the S/N ratio of the erosion rate is found to be -49.02 db. Figure 5.1 shows graphically the effect of the five control factors on erosion rate. The analysis is made using the popular software specifically used for design of experiment applications known as MINITAB 14. Before any attempt is made to use this simple model as a predictor for the measures of performance, the possible interactions between the control factors must be considered. Thus factorial design incorporates a simple means of testing for the presence of the interaction effects. Analysis of the result leads to the conclusion that factor combination of A_1, B_2, C_3, D_2 and E_2 gives minimum erosion rate. As for as minimization of erosion rate is concerned, factors A, B, D and E have significant effect whereas factor C has least effect as shown in Figure 5.1. It is also observed from figure 5.1 that the significant level of each factor for minimization of erosion rate. Similarly Figures

5.2, 5.3 and 5.4 shows the interaction graphs for A×B, A×C and B×C for erosion rate respectively.

Table 5.1. Experimental design using L_{27} orthogonal array

Expt. No.	Impact velocity (A)m/sec	Fiber content (B) %	Stand-off Distance (C) mm	Impingement angle (D)Degree	Erodent size (E) µm	Erosion rate (Er)mg/kg	S/N ratio (db)
1	45	30	120	30	400	290.43	-49.26
2	45	30	180	60	500	245.45	-47.8
3	45	30	240	90	600	226.34	-47.1
4	45	40	120	60	500	195.71	-45.83
5	45	40	180	90	600	282.84	-49.03
6	45	40	240	30	400	264.94	-48.46
7	45	50	120	90	600	394.12	-51.91
8	45	50	180	30	400	281.42	-48.99
9	45	50	240	60	500	178.58	-45.04
10	65	30	120	60	600	325.61	-50.25
11	65	30	180	90	400	356.88	-51.05
12	65	30	240	30	500	245.43	-47.8
13	65	40	120	90	400	249.45	-47.94
14	65	40	180	30	500	258.83	-48.26
15	65	40	240	60	600	242.16	-47.68
16	65	50	120	30	500	234.75	-47.41
17	65	50	180	60	600	339.37	-50.61
18	65	50	240	90	400	378.19	-51.55
19	85	30	120	90	500	407.20	-52.2
20	85	30	180	30	600	228.26	-47.17
21	85	30	240	60	400	246.19	-47.83
22	85	40	120	30	600	268.49	-48.58
23	85	40	180	60	400	332.80	-50.44
24	85	40	240	90	500	208.56	-46.38
25	85	50	120	60	400	352.17	-50.94
26	85	50	180	90	500	420.58	-52.48
27	85	50	240	30	600	369.54	-51.35

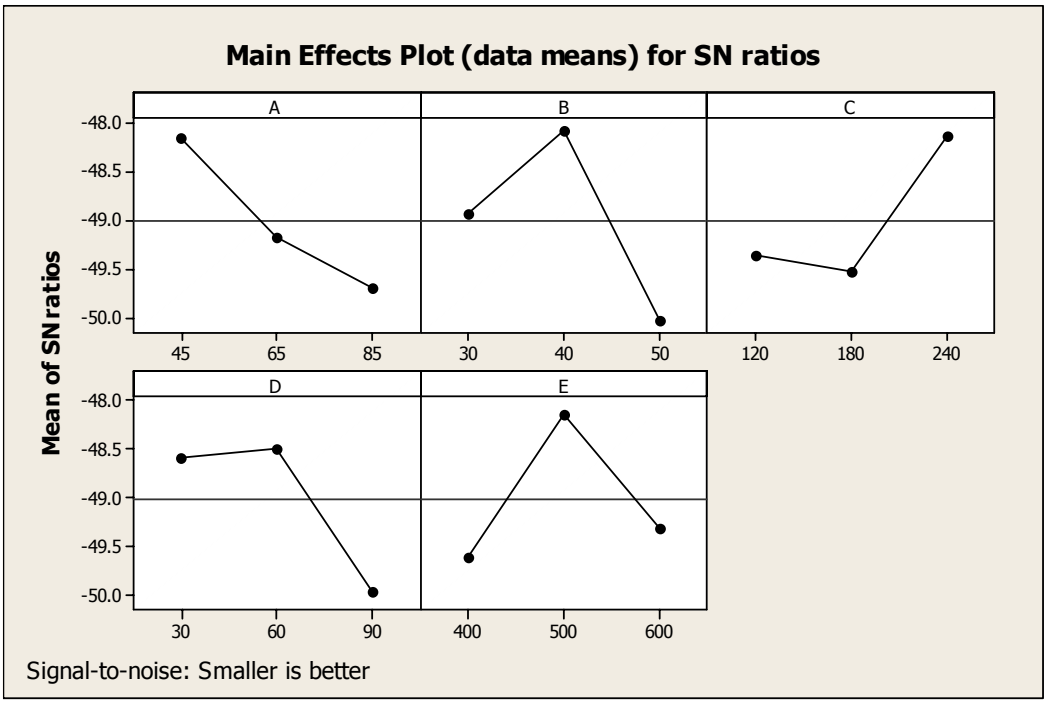

Figure 5.1. Effect of control factors on erosion rate

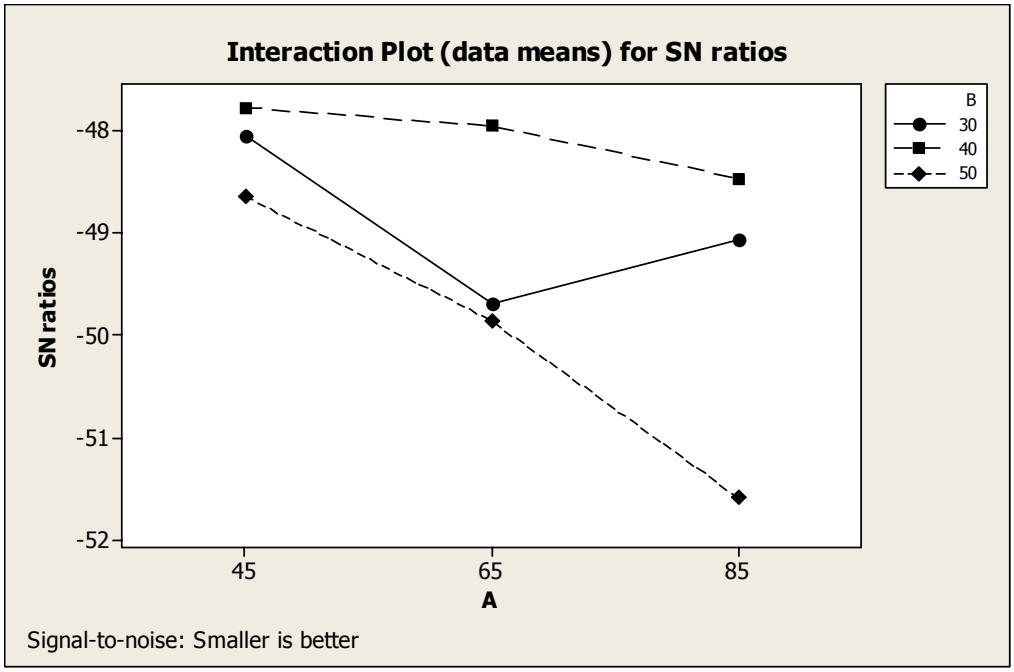

Figure 5.2. Interaction graph between A×B for erosion rate

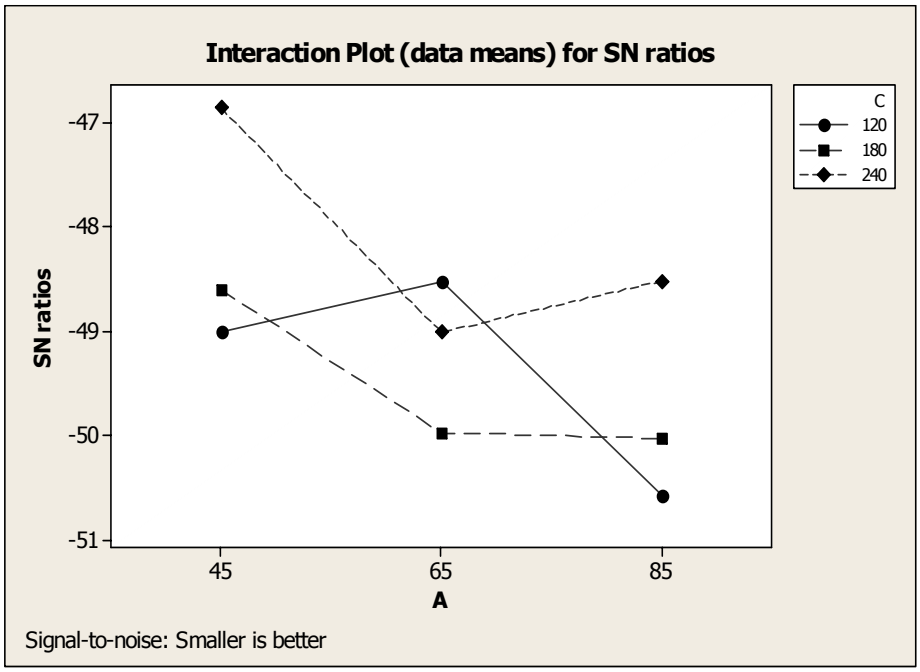

Figure 5.3. Interaction graph between A×C for erosion rate

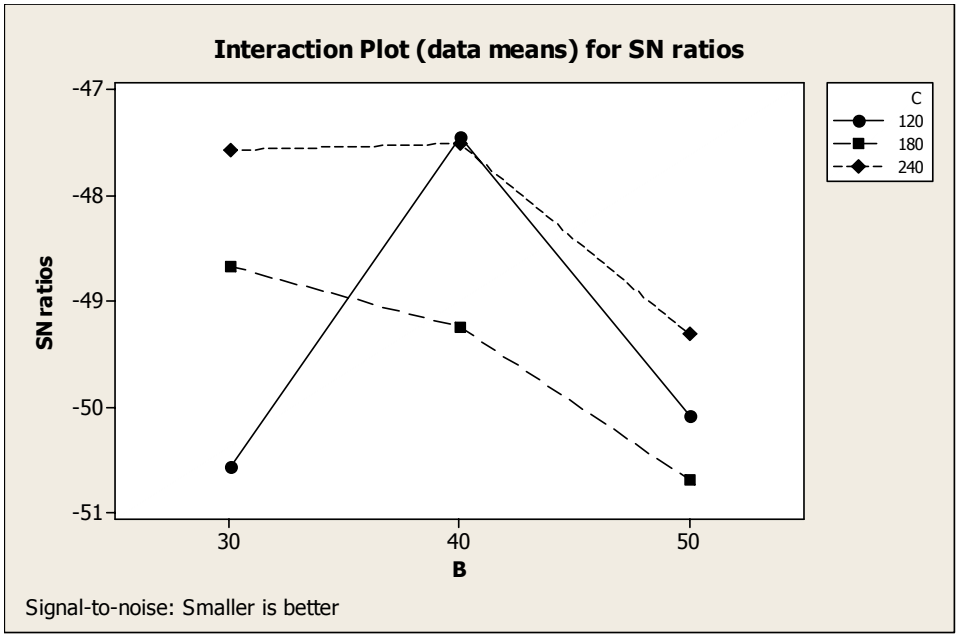

Figure 5.4. Interaction graph between B×C for erosion rate

The experimental erosion wear rate (E_{expt}) of the TiO_2 filled glass fiber reinforced epoxy composites are calculated as given in Table 5.1. Seventy five percent of data collected from erosion test is used for training whereas twenty five percent data is used for testing. The parameters of three layer architecture of ANN model are set as input nodes = 5, output node

= 1, hidden nodes = 12, learning rate = 0.01, momentum parameter = 0.03, number of epochs = 20, 0000 and a set of predicted output (E_{rANN}) is obtained. Table 5.2 presents a comparison between the experimental and the ANN predicted results. The errors calculated with respect to the theoretical results are also given.

Table 5.2. Comparison of experimental result and ANN results

Expt. No.	$E_{rexpt.}$ (mg/kg)	E_{rANN} (mg/kg)	Error (%)
1	290.43	245.33	6.85191
2	245.45	203.95	9.57425
3	226.34	176.93	6.88787
4	195.71	111.31	9.91262
5	282.84	230.34	4.41946
6	264.94	204.54	1.73624
7	394.12	286.33	10.8571
8	281.42	193.51	8.14085
9	178.58	127.07	7.55404
10	325.61	224.53	11.0807
11	356.88	302.1	2.86371
12	245.43	173.76	2.71767
13	249.45	168.65	6.33393
14	258.83	186.49	2.83583
15	242.16	156.04	8.72150
16	234.75	178.27	3.62939
17	339.37	262.33	3.54775
18	378.19	286.06	7.17364
19	407.20	307.29	8.57318
20	228.26	183.82	9.00727
21	246.19	171.43	3.96441
22	268.49	233.62	11.2224
23	332.80	232.37	10.6461
24	208.56	164.48	10.0307
25	352.17	264.4	6.46562
26	420.58	326.23	6.97845
27	369.54	298.25	1.70211

It is observed that maximum error between ANN prediction and experimental wear rate is 0-12%. The error in case of ANN model can further be reduced if number of test patterns is increased. However, present study demonstrates application of ANN for prediction of wear rate in a complex process of solid particle erosion of polymer composites.

5.2. Steady State Erosion

Erosion behaviour of the composites is generally ascertained by correlating erosion rate with impingement angle, erodent velocity and erodent particle size. Erosion behaviour strongly depends on impingement angle. Ductile behaviour is characterized by maximum erosion rate and generally occurs at 15–30^0. Brittle behaviour is characterized by maximum erosion rate at 90^0. Semi-ductile behaviour is characterized by the maximum erosion rate at 45-60^0. Thus the erosion wear behaviour of polymer composites can be grouped into ductile and brittle categories although this grouping is not definitive because the erosion characteristics equally depend on the experimental conditions as on composition of the target material. The results are presented in Figure 5.5 which shows the peak erosion taking place at an impingement angle of 60^0 for the filled composites. This clearly indicates that these composites respond to solid particle impact neither in a purely shows semi-ductile behaviour as per literature. This behaviour can be termed as semi-ductile in nature which may be attributed to the incorporation of glass fibers and TiO_2 particles within the epoxy body.

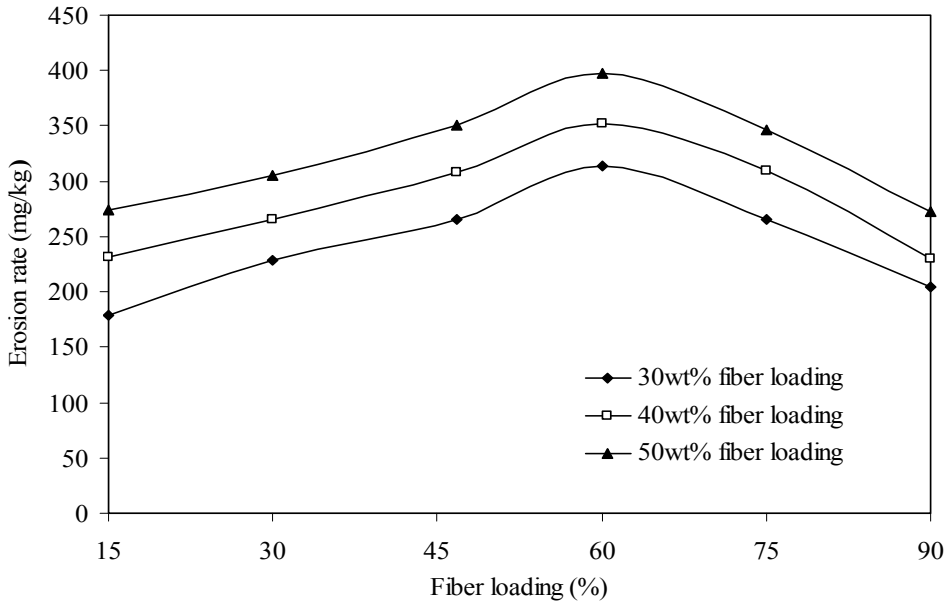

Figure 5.5. Variation of erosion rate with impingement angle

5.3. Surface morphology of the composites

Generally surface morphology of eroded surfaces indicates whether erosion has occurred by a ductile or brittle mechanism. Hence scanning electron microscopy (SEM) studies have been done to ascertain the wear mechanism at 30^0, 60^0 and 90^0 impact angles. Figure 5.6 show micrographs of eroded surfaces of 30wt% of the composite at 30^0 impact angles at impact velocity of 65 m/s. It is evident from the micrographs (Figure 5.6a, b) that the material removal in composite with 30wt% fiber loading is dominated by microploughing, micro-cutting and plastic deformation. The plastically deformed material subsequently removed from the surface by micro-cutting leads to maximum wear at 30^0 impact angle; most material is lost when a maximum strain in the target is exceeded. Under normal impact, formation of micro-cracks and embedment of fragments of sand particles in composite with 40wt% fiber loading is evident from the micrographs (Figure 5.7). Micrograph (Figure 5.7a, b) confirms the brittle nature of the composite with deeper micro-cracks. However, the normal impact did not result in higher erosion rate like brittle materials. During normal impact the largest part of the initial energy is converted in to heat and hence matrix is softened which resulted in embedment of sand particles (Figure 5.6). The embedded sand particles control the further erosion of the target surface.

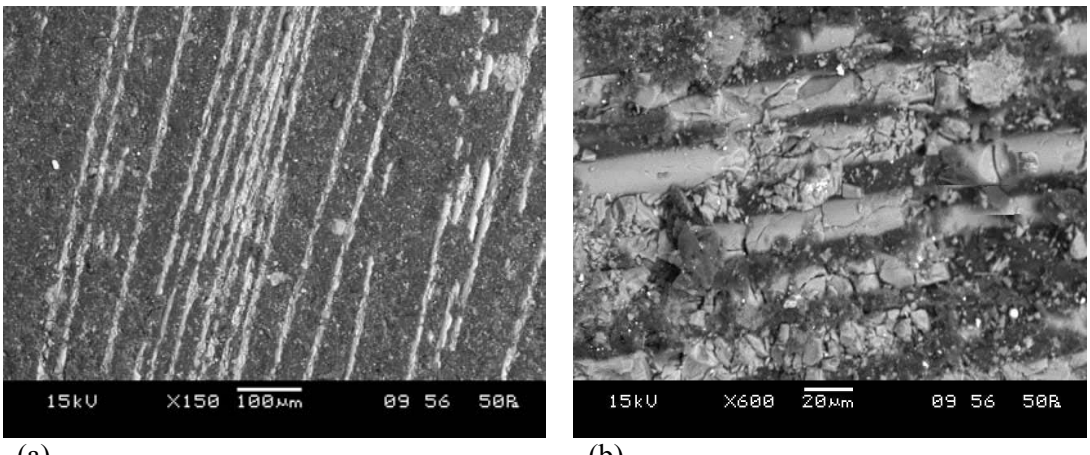

(a) (b)

Figure 5.6. Scanning electron micrograph of 30wt% fiber loading composite

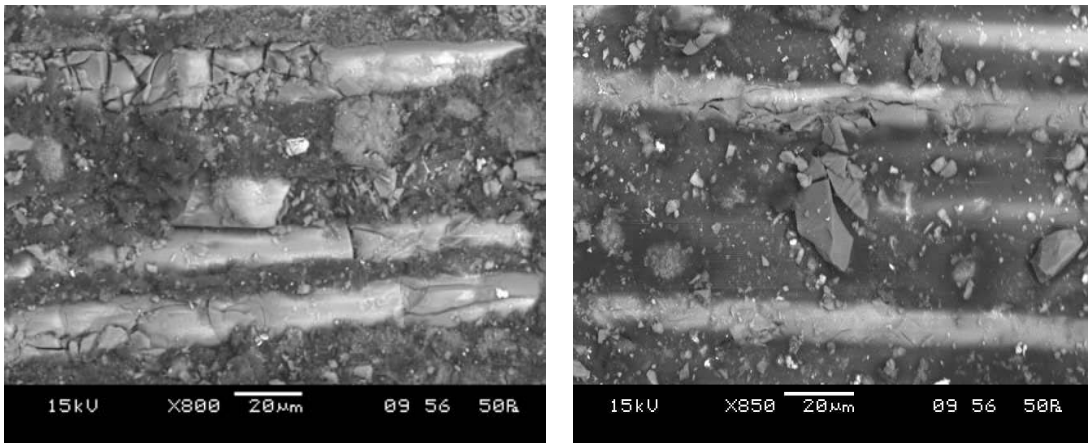

(a) (b)

Figure 5.7. Scanning electron micrograph of 40wt% fiber loading composite

Figure 5.8a, b show micrographs of eroded surfaces of 50wt% glass fiber reinforced epoxy composite. At oblique impact angle, micrographs (Figure 5.8a) shows matrix is plastically deformed and amount of deformation is proportional to impact velocity of particles. At lower impact velocity removal of matrix along the length of the fiber and subsequently exposed fiber getting removed can be seen from the micrograph (Fig. 5.8b).

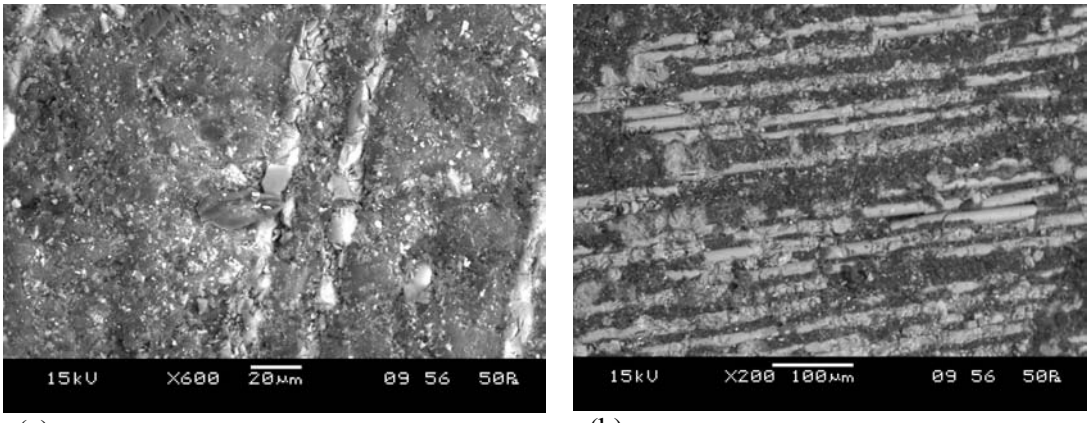

(a) (b)

Figure 5.8. Scanning electron micrograph of 50wt% fiber loading composite

5.4. ANOVA and the effects of factors

In order to understand a concrete visualization of impact of various factors and their interactions, it is desirable to develop analysis of variance (ANOVA) table to find out the order of significant factors as well as interactions. Table 5.3 shows the results of the ANOVA with the erosion rate. This analysis was undertaken for a level of confidence of significance of 5 %. The last column of the table indicates that the main effects are highly significant (all have very small p-values).

From Table 5.3, one can observe that the fiber content (p=0.270), angle of impingement (p=0.369), velocity of impact (p=0.394) and erodent size (p=0.401) have great influence on erosion rate. The interaction between fiber loading × stand-off distance (p=0.654) and impact velocity × stand-off distance (p=0.814) show significance of contribution on the erosion rate and the factor stand-off distance (p=0. 409) and impact velocity ×fiber loading (p=0.823) present less significance of contribution on erosion rate. As impact velocity and fiber loading interaction is less significant but it can not be neglected because both impact velocity and fiber loading is more significant individual.

Table 5.3. ANOVA table for erosion rate

Source	DF	Seq SS	Adj SS	Seq MS	F	P
A	2	11.153	11.153	5.577	1.19	0.394
B	2	17.413	17.413	8.707	1.85	0.270
C	2	10.586	10.586	5.293	1.13	0.409
D	2	12.156	12.156	6.078	1.29	0.369
E	2	10.876	10.876	5.438	1.16	0.401
A*B	4	6.894	6.894	1.724	0.37	0.823
A*C	4	7.160	7.160	1.790	0.38	0.814
B*C	4	12.304	12.304	3.076	0.65	0.654
Error	4	18.807	18.807	4.702		
Total	26	107.349				

5.5. Confirmation xperiment

The optimal combination of control factors has been determined in the previous analysis. However, the final step in any design of experiment approach is to predict and verify improvements in observed values through the use of the optimal combination level of control factors. The confirmation experiment is performed by conducting a new set of factor combination $A_2B_3D_1E_3$ but factor C has been omitted because factor C and interaction $A \times C$ and $B \times C$ have least effect on erosion rate as evident from Table 5.3. The estimated S/N ratio for erosion rate can be calculated with the help of following prediction equation:

$$\bar{\eta}_1 = \bar{T} + (\bar{A}_2 - \bar{T}) + (\bar{B}_3 - \bar{T}) + [(\bar{A}_2\bar{B}_3 - \bar{T}) - (\bar{A}_2 - \bar{T}) - (\bar{B}_3 - \bar{T})] + (\bar{D}_1 - \bar{T}) + (\bar{E}_3 - \bar{T}) \quad (6)$$

$\bar{\eta}_1$ Predicted average

$\bar{T}$ Overall experimental average

$\bar{A}_2, B_3, \bar{D}_1$ and $\bar{E}_3$ Mean response for factors and interactions at designated levels.

By combining like terms, the equation reduces to

$$\bar{\eta}_1 = \bar{A}_2\bar{B}_3 + \bar{D}_1 + \bar{E}_3 - 2\bar{T} \quad (7)$$

A new combination of factor levels A_2, B_3, D_1 and E_3 is used to predict deposition rate through prediction equation and it is found to be $\bar{\eta}_1$ = -49.72db

For each performance measure, an experiment is conducted for a different factors combination and compared with the result obtained from the predictive equation as shown in Table 5.4.

Table 5.4. Results of the confirmation experiments for Erosion rate

	Optimal control parameters	
	Prediction	Experimental
Level	$A_2B_3D_1E_3$	$A_2B_3D_1E_3$
S/N ratio for Erosion rate (mg/kg)	-49.72	-46.95

The resulting model seems to be capable of predicting erosion rate to a reasonable accuracy. An error of 5.86 % for the S/N ratio of erosion rate is observed. However, the error can be further reduced if the number of measurements is increased. This validates the development of the mathematical model for predicting the measures of performance based on knowledge of the input parameters.

******

CHAPTER 6

CONCLUSIONS

This analytical and experimental investigation into the erosion behaviour of TiO_2 filled glass-epoxy composites leads to the following conclusions:

- This work shows that successful fabrication of a glass fiber reinforced epoxy composites filled with micro-sized TiO_2 is possible by simple hand lay-up technique.
- It is noticed that there is significant improvement in the mechanical properties of the composites with the increase in fiber loading. The micro-hardness, density and flexural properties of the composites are also greatly influenced by the content of fibres.
- Solid particle erosion characteristics of these composites can be successfully analyzed using Taguchi experimental design scheme. Taguchi method provides a simple, systematic and efficient methodology for the optimization of the control factors.
- Study of influence of impingement angle on erosion rate of the composites with different percentage of fiber loading reveals their semi-ductile nature with respect to erosion wear. The peak erosion rate is found to be occurring at 60^0 impingement angle under the various experimental conditions.
- SEM studies reveal that material removal takes place by microcutting, plastic deformation, and micro-cracking, exposure of fibers and removal of the fiber.
- Artificial neural network technique has been applied to predict the erosion rate of composites. The results show that the predicted data are well acceptable when comparing them to measured values. The predicted property profiles as a function of fiber content and testing conditions proved a remarkable capability of well-trained neural networks for modelling concern.

6.1. Scope for Future Work

Solid particle erosion study of other types of glass fiber except E-glass fiber reinforced with polyester or epoxy resin composites filled with ceramic filler has been a less studied area. There is a very wide scope for future scholars to explore this area of research. In future, this study can be extended to new hybrid composites using other potential fillers and the resulting experimental findings can be similarly analyzed.

******

REFERENCES

1. Agarwal, B. D and Broutman, L. J, (1990). Analysis and Performance of Fiber Composites, Second Edition, Jhon Wiley & Sons, Inc. New York.
2. Gregory Sawyer W, Freudenberg Kevin D, Bhimaraj Pravee and Schadler Linda S, (2003). A study on the friction and wear behavior of PTFE filled with alumina nanoparticles, Wear, 254, pp. 573-580.
3. Jung-il K., Kang P.H and Nho Y.C, (2004). Positive temperature coefficient behavior of polymer composites having a high melting temperature, J Appl Poly Sci., 92, pp. 394-401.
4. Nikkeshi S, Kudo M and Masuko, T, (1998). Dynamic viscoelastic properties and thermal properties of powder-epoxy resin composites, J Appl Poly Sci., 69, pp. 2593-2598.
5. Zhu, K and Schmauder, S, (2003). Prediction of the failure properties of short fiber reinforced composites with metal and polymer matrix, Comput Mater Sci. 28, pp. 743-748.
6. Rusu M, Sofian N and Rusu D, (2001). Mechanical and thermal properties of zinc powder filled high density polyethylene composites, Polym Test, 20, pp. 409-417.
7. Tavman I. H, (1997). Thermal and mechanical properties of copper powder filled poly (ethylene) composites, Powder Technol, 91, pp. 63-67.
8. Rothon R.N, (1997). Mineral fillers in thermoplastics: filler manufacture, J Adhesion, 64, pp. 87-109.
9. Rothon R.N, (1999). Mineral fillers in thermoplastics: filler manufacture and characterization. Adv. Polym. Sci. 139, pp. 67-107.
10. Bonner W.H, (1962). U.S. Patent 3,065,205.

11. Stokes V.K, Inzinna L.P, Liang E.W, Trantina G.G and Woods J.T, (2000). A phenomenological study of the mechanical properties of long fiber filled injection-molded thermoplastic composites. Polym Compos., 21(5), pp. 696-710.
12. Srivastava V.K, Prakash R and Shembekar P.S, (1988). Fracture behaviour of fly ash filled FRP composites. Compos Struct., 10, pp. 271-279.
13. Srivastava V.K and Shembekar P.S, (1990). Tensile and fracture properties of epoxy resin filled with flyash particles. J Mater Sci., 25, pp. 3513-3516.
14. Tilly G. P,(1969). Erosion caused by airborne particles, Wear, 14(1), pp. 63-79.
15. Zahavi J, Nadiv S and Schmitt Jr G. F, (1981). Indirect damage in composite materials due to raindrop impact, Wear, 72(3), pp. 305-313.
16. Tilly G. P and Wendy Sage, (1970). The interaction of particle and material behaviour in erosion processes, Wear, 16(6), pp. 447-465.
17. Pool K.V, Dharan C.K.H, and Finnie I, (1986). Erosion wear of composite materials, wear, vol. 107,pp. 1-12
18. Tsiang T.H,(1989).Sand erosion of fiber composites: Testing and evaluation in CC. Chamis (Ed.), Test methods for design allowables for fibrous composites, Vol. 2, American Society for Testing and Materials, (ASTM) STP I003, Philadelphia, pp. 55-74.
19. Mathias P-J., Wu W, Goretta K.C, Routbort L.J, Groppi D.P and Karasek K.R, (1989). Solid particle erosion of a graphite-fiber reinforced bismaleimide polymer composite, Wear, I35, pp. 161-169.
20. Karasek, K.R, Goretta, K.C, Helberg, D.A and Routbort, J.L, (1992). Erosion in bismaleimide polymers and bismaleimide polymer composites, J. Mater. Sci. Lett. 11, pp. 1143-1144.

21. Tilly G.P, (1969). Sand erosion of metals and plastics: A brief review, Wear, 14(4), pp. 241-248.
22. Tilly G.P. (1979). Erosion caused by impact of solid particles. In: Scott D, editor. Treatise on materials science and technology, 13, pp. 28-37.
23. Arnold J.C and Hutchings I.M. (1990). The mechanisms of erosion of unfilled elastomers by solid particle impact. Wear, 138, pp. 33-46.
24. Arnold J.C and Hutchings I.M. (1989). Flux rate effects in the erosive wear of elastomers. J Mater Sci., 24, pp. 833-839.
25. Friedrich K, (1986). Erosive wear of polymer surfaces by steel ball blasting. J Mater Sci., 21, pp. 3317-3332.
26. Zahavi J. (1981). Solid particle erosion of polymeric coatings. Wear; 71, pp. 191-210.
27. Williams Jr. J.H and Lau KE. (1974). Solid particle erosion of graphite epoxy composites. Wear, 29, pp. 219-230.
28. Dhar S, Krajac T, Ciampini D and Papini M, (2005).Erosion mechanisms due to impact of single angular particles, Wear, 258(1-4), pp. 567-579.
29. Gomes Ferreira C, Ciampini D and Papini M, (2004). The effect of inter-particle collisions in erosive streams on the distribution of energy flux incident to a flat surface, Tribology International, 37, pp. 791-807.
30. Tilly G.P, (1973). A two stage mechanisms of ductile erosion. Wear, 23, pp.87-96.
31. Wiederhorn S.M and Hockey B.J, (1983). Effect of material parameters on the erosion resistance of brittle materials. J Mater Sci., 18, pp. 766-780.
32. Scattergood R.O and Routbort J.L, (1981). Velocity and size dependence of the erosion rate in silicon. Wear, 67, pp. 227.
33. Thai C.M, Tsuda K and Hojo H, (1981). Erosion behaviour of polystyrene. J Test Eval, 9(6), pp. 359-365.

34. Karasek K.R, Goretta K.C, Helberg D.A and Rourbort J.L. (1992). Erosion in bismaleimide polymers and bismaleimide-polymer composites. J Mater Sci Lett; 11, pp. 1143-1144.
35. Rao P.V and Buckley D.H, (1985). Angular particle impingement studies of thermoplastic materials at normal incidence. ASLE Trans, 29(3), pp. 283-298.
36. John Rajesh J, Bijwe J, Tewri U.S and Venkataramanan B, (2001). Erosive wear of various polyamides. Wear, 249(8), pp. 702-714.
37. Zahavi J and Schmitt Jr. G. F, (1981). Solid particle erosion of reinforced composite materials, Wear, 71, pp. 179-190.
38. Ruff A.W and Wiederhorn S.M. (1979). Erosion by solid particle impact. In: Preece CM, editor. Treatise on materials science and technology, vol. 16. New York: Academic Press., pp. 69-125.
39. Preece C.M and Macmillan N.H, (1977). EROSION, Annual Review of Materials Science, 7, pp. 95-121.
40. Sundararajan G, (1983). The solid particle erosion of metals and alloys. Trans. Indian Inst. Met. 36(6), pp. 474-495.
41. Zum Gahr K. H, (1987). Microstructure and Wear of Materials, tribology Series, Vol. 10, Elsevier, Amsterdam.
42. Kruschov M.M. (1974). Principles of abrasive wear**,** Wear, 28, pp. 69-88.
43. Murray M. J, Watson J. D, Mutton P and Ludema K. C, (ed.), (1979). Proc. Int. Conf. on Wear of Materials, American Society of Mechanical Engineers, New York, pp. 257.
44. Richardson R. C. D, (1967). The maximum hardness of strained surfaces and the abrasive wear of metals and alloys, Wear, 10(5), pp. 353-382.

45. Ericson F, Johansson S and Schweitz, J.-Å. (1988). Hardness and fracture toughness of semiconducting materials studied by indentation and erosion techniques. Mater. Sci. Eng. A: 105/106, pp. 131-141.
46. Wiederhorn M and Hockey B. J, (1980). Effect of material parameters on the erosion resistance of brittle materials, J. Mater. Sci., 18, pp. 766-780.
47. Friedrich K and Ludema K. C, (ed.), (1987). Proc. Int. Conf. on wear of Materials, American Society of Mechanical Engineers, New York, pp. 833.
48. Lamy B, (1984). Effect of brittleness index and sliding speed on the morphology of surface scratching in abrasive or erosive processes, Tribol. Int., 17(1), pp. 35-38.
49. Briscoe, B, (1981). Wear of Polymers-An Essay on Fundamental-Aspects, Tribol Int, 14, pp. 231-243.
50. Miyazaki N and Hamao T, (1994). Solid particle erosion of thermoplastic resins reinforced by short fibers, J. Compos. Mater., 28 (9), pp. 871-883.
51. Haraki N, Tsuda K and Hojo H, (1992). Sand erosion behaviour of composites reinforced with glass cloth laminates, Adv. Compos. Lett., 1 (1), pp. 31-33.
52. Lhymn C and Lhymn Y.O, (1989). Erosive wear of fibrous PEEK composites, in: Proceedings of the 21st International SAMPE Technical Conference, Eric, PA, USA, 25-28 September, 720-729.
53. Hovis S.K, Talia J.E and Scattergood R.O, (1986). Erosion in multiphase systems, Wear, 108, pp. 139-155.
54. Ballout Y.A, Hovis S.K and Talia J.E, (1990). Erosion in glass–fiber reinforced epoxy composite, Scripta Metallurgicaet materialia, 24, pp. 195-200.
55. El-Tayeb N.S.M and Yousif B.F, (2007). Evaluation of glass fibre reinforced polyester composite for multi-pass abrasive wear applications, Int. J. Wear, 262, pp. 1140-1151.

56. Zum Gahr K.-H, (1987). Microstructure and wear of materials, Tribology Series 10, Elsevier, Amsterdam.

57. Glen, S. P, (1993). Taguchi Methods: A Hands-on Approach, Addison-Wesley.

58. Rajasekaran, S and Vijayalakshmi Pai G. A, (2003). Neural Networks, Fuzzy Logic And Genetic Algorithms-Synthesis and Applications, Prentice Hall of India Pvt. Ltd., New Delhi.

59. Rao V and Rao H, (2000). C++ Neural Networks and Fuzzy Systems, BPB Publications.

******